Ultra-compact visible light depolarizer based on dielectric metasurface

Yilin Wang[1], Wenqi Zhu[2,3], Cheng Zhang[2,3,*], Qingbin Fan[1], Lu Chen[2,3], Henri Lezec[2], Amit Agrawal[2,3], and Ting Xu[1,*]

1. *National Laboratory of Solid State Microstructures, College of Engineering and Applied Sciences and Collaborative Innovation Center of Advanced Microstructures, Nanjing University 210093, China*
2. *Physics Measurement Laboratory, National Institute of Standards and Technology, Gaithersburg, Maryland 20899, United States*
3. *Maryland NanoCenter, University of Maryland, College Park, Maryland 20742, United States*

Abstract

With rapid development towards shrinking the size of traditional photonic systems such as cameras, spectrometers, displays and illumination systems, there is an urgent need for high performance and ultra-compact functional optical elements. The large footprint of traditional bulky optical elements, their monofunctional response and the inability for direct integration into nanophotonic devices have severely limited progress in this area. Metasurfaces, consisting of an array of subwavelength nanoscatterers with spatially varying geometries, have shown remarkable performance as ultrathin multifunctional optical elements. Here, based on an all-dielectric metasurface, we propose and experimentally

demonstrate a spatial domain optical depolarizer capable of efficiently depolarizing linearly polarized light in the visible spectral band from 450 nm to 670 nm, with a degree of polarization of less than 10 %. Remarkably, it is capable of depolarizing light beam with a diameter down to several micrometers, about two orders of magnitude smaller than commercial liquid crystal depolarizers. Furthermore, the long response time, bulky footprint, tight optical alignment tolerance and large pixel size severely limit the performance and system integration of commercial depolarizers. We envision the metasurface depolarizer to find applications in next generation ultra-compact grating spectrometers and illumination systems.

State of polarization (SOP) is one of the fundamental property of light. However, for certain applications, such as in grating spectrometers for spectral characterization and imaging, a linearly polarized input beam is not ideal, and affects the measurement accuracy. An optical depolarizer can reduce the degree of polarization (DOP) of a highly-polarized beam. As early as in 1928, a passive depolarizer was first described by Lyot [1]. It consisted of two birefringent crystals aligned at an angle of 45 degree between the two optical axes, and can only work for illumination with broadband incoherent light. With the development of laser technology in the late 20^{th} century, more attention was paid towards developing optical depolarizers working with coherent monochromatic light. For example, Billings succeeded in depolarizing monochromatic light with a temporally varying retarder based on dynamic depolarization technique of

rapidly changing the SOP of light [2]. However, this technique cannot be applied to ultrafast optical applications with short time constants. Since the beginning of 21st century, various liquid crystal (LC) depolarizers have been reported [3-4]. The primary limitation of commercial LC depolarizers is their large pixel size, which makes them only applicable for use with incident beams of diameters in the millimeter-scale. Moreover, these devices are bulky making them difficult for further integration in ultra-compact optical systems including with photonic integrated circuits.

In recent years, metasurfaces, consisting of an array of subwavelength nanoscatterers with spatially varying geometries engineered to perform specific optical functions, have shown excellent performance in their ability to manipulate the amplitude, phase, and polarization of light [5-10]. Compact planar footprint, ease-of-integration and high diffraction efficiencies are some of the notable characteristics that merit their applicability across a variety of optical applications including high numerical aperture lensing, hologram generation and polarimetry [11-20]. In principle, since metasufaces are able to fully control the propagation of light at subwavelength scale, they can also be used for designing novel optical depolarizers. Preliminary works utilizing plasmonic nanoantennas and random corrugated gratings have explored their potential as depolarizers [21-22]. However, employment of lossy metal as the constituent material significantly reduces the devices' conversion efficiencies, which further restricts their practical application.

Here, we propose and experimentally demonstrate an all-dielectric metasurface depolarizer capable of depolarizing linearly polarized light with DOP less than 10 %

over a broad visible frequency spectral range (λ_0 = 450 nm to 670 nm). Since the metasurface depolarizer consists of subwavelength nanoscatterers (nanopillar in-plane dimensions < λ_0) and has extremely high pixel density (pitch ≈ λ_0), it can depolarize a beam with a diameter down to ≈ 10 μm, which is about two orders of magnitude smaller than commercial LC depolarizer. We anticipate that this device can be used as an ultra-compact platform for integration with polarization independent nanophotonic devices.

Figure 1a shows the schematic diagram of the proposed metasurface depolarizer consisting of an array of TiO_2 nanopillars, designed to act as nanoscale half waveplates, on a SiO_2 substrate. Upon normal incidence illumination with a linearly polarized light, and with the incident electric-field oriented at an angle of α with respect to the optical axis of a given nanopillar, the polarization direction upon transmission is rotated by an angle 2α towards the optical axis, akin to a half waveplate. Here, we choose the optical axis of each constituent TiO_2 nanopillar to be random such that, upon transmission, an incident linearly polarized light can be transformed into a mixture of random polarization directions thereby significantly reducing its DOP. To further quantify the performance of the depolarizer, we define DOP as:

$$\mathrm{DOP} = \frac{\sqrt{Q^2+U^2+V^2}}{I} \times 100\% \quad (1)$$

where I, Q, U, V are the four fundamental parameters of the Stokes vector $\boldsymbol{S}$, among which I is the total light intensity. When a beam passes through the metasurface element, the Stokes vector turns from $\mathbf{S}_{\mathrm{in}} = (I, Q, U, V)^T$ to $\mathbf{S}_{\mathrm{out}} = (I', Q', U', V')^T$, related by a 4×4 real matrix $\mathbf{M}$ as:

$$\mathbf{S}_{\mathrm{out}} = \mathbf{M}\mathbf{S}_{\mathrm{in}} \quad (2)$$

Here **M** is the Mueller matrix of the metasurface element having the form:

$$\mathbf{M} = \begin{bmatrix} 1 & 0 & 0 & 0 \\ 0 & cos\,4\theta & sin\,4\theta & 0 \\ 0 & sin\,4\theta & -cos\,4\theta & 0 \\ 0 & 0 & 0 & -1 \end{bmatrix} \tag{3}$$

where θ is the rotation angle between the long axis of nanopillar and the x axis. For a linearly polarized light, the Stokes vector of the outgoing beam $\mathbf{S}_{\text{out}}$ can be written as:

$$\mathbf{S}_{\text{out}} = \begin{bmatrix} I' \\ Q' \\ U' \\ V' \end{bmatrix} = \begin{bmatrix} 1 \\ \frac{1}{N}\sum_{n=1}^{N}\cos(4\theta_n - 2\alpha) \\ \frac{1}{N}\sum_{n=1}^{N}\sin(4\theta_n - 2\alpha) \\ 0 \end{bmatrix} \tag{4}$$

Here, N is the number of nanopillars composing the metasurface depolarizer, θ_n is the rotation angle of nth nanopillar. According to eq. 4, when N is sufficiently large, Q' and U' will approach to zero, which indicates that the metasurface element will be effective for light depolarization.

The metasurface depolarizer designed for this work is composed of a series of randomly orientated rectangular nanopillars with a lattice constant of P = 450 nm. TiO_2 is chosen as metasurface constituent material because of its large index of refraction and low loss at visible wavelengths [23]. For an identical height h = 600 nm of the TiO_2 nanopillars, we tailor their in-plane cross-sectional dimensions along with two orthogonal directions D_x and D_y, such that each unit cell can act as a half waveplate. Fig.1(b) reveals the finite-difference time-domain (FDTD) simulated polarization conversion efficiency and phase difference of light in the spectral range between 450 nm and 670 nm, with the optimized structural parameters D_x = 120 nm and D_y = 335 nm. Here, cross-polarization and co-polarization conversion efficiencies are respectively defined as the ratio of transmitted power of the right- and left-handed

circularly polarized light to that of the incident left-handed circularly polarized light. The nanopillars co-polarization conversion efficiency is relatively low, smaller than 5 %, which is a prerequisite for efficient broadband depolarization of linearly polarized light. In addition, it is worth noting that phase difference is close to π over the entire visible band, which means that this structure can realize the function of a half waveplate over a broad spectral range.

Figure 2(a)-(c) gives the optical and scanning electron microscope (SEM) images of the fabricated metasurface depolarizer with a diameter of 450 μm. The detailed fabrication process is reported elsewhere [24]. The experimental setup used to characterize the depolarizing performance of the metasurface device is shown in Fig.2(d). Linearly polarized light filtered from a broadband supercontinuum laser is normally incident onto the metasurface from the substrate side. A low numerical aperture objective lens is used to reduce the beam size. The DOP of the transmitted light at various wavelengths in the visible range selected using a filter is directly measured using an optical polarimeter.

The experimental measurement results are summarized in Fig. 3. At the wavelength of 532 nm, Fig.3(a) gives the measured DOP of transmitted beam through the metasurface as a function of incident polarization rotation angle at a step of 15°. Compared with a DOP of 99.97 % of the incident linear polarized light, it can be seen that the DOPs of depolarized light are all < 6 % for the various rotation angles, reaching a minimum value of ≈ 2.5 %, which indicates the excellent polarization-insensitive response of the metasurface depolarizer. The transmission efficiency of the

metasurface depolarizer is ≈ 60 % which is much higher than that of plasmonic depolarizers [21-22]. In addition to the polarization rotation angle, the DOP values are also measured as a function of incident angle of the laser beam with respect to surface normal of the metasurface sample, varying from -30° to 30° at a step of 10°. The DOP values are found to not vary much and stay between ≈ 3 % to ≈ 6 %, as a function of the incident angle (Fig. 3(b)). Next, we investigate the depolarization effect on the incident beam diameter, as illustrated in Fig. 3(c). Upon decreasing the incident beam diameter from 200 μm to 10 μm, the DOP value monotonically increases slightly from ≈ 4 % to ≈ 9 %. Remarkably for a beam diameter of 10 μm, a DOP value of < 10 % can still be obtained, which is more than two orders of magnitude smaller than that of commercial LC depolarizer. Finally, Fig. 3(d) shows the depolarizer measurements over a broad range of wavelengths spanning the visible range. As expected, the device has a similar depolarization effect for seven different visible wavelengths within DOP < 6 % for each. These results imply that the compact metasurface depolarizer platform demonstrated here offers high performance over a wide range of incident angles and visible wavelengths, and can efficiently depolarize laser beams of ultra-small diameters.

In conclusion, we have demonstrated a spatial domain all-dielectric metasurface depolarizer consisting of randomly oriented rectangular TiO_2 nanopillars exhibiting efficient performance over the entire visible spectral range. The wavelength range of operation can be easily tuned to a different spectral range (from the deep-ultraviolet to the terahertz) by choosing a different constituent material and scaling the nanopillar

dimensions. The compact and ultrathin configuration of the metasurface lends itself towards further integration in small-footprint optical devices and systems, and this technology may eventually find broader applications in the nano-optics field.

Acknowledgement

The work was supported in part by the National Key R&D Program of China (Grant Nos. 2017YFA0303700 and 2016YFA0202100), the National Natural Science Foundation of China (Grant Nos. 61575092 and 11774163). T.X. acknowledges support from the Fundamental Research Funds for the Central Universities.

References

[1] Lyot, A. Recherches sur la polarisation de la lumière des planètes et de quelques substances terrestres. Ann. Obs. Paris **8**, 100–104 (1929).

[2] Billings, B. H. A Monochromatic Depolarizer. J. Opt. Soc. Am. **41**, 966-968 (1951).

[3] Diorio, N. J., Fisch, M. R., West, J. L. Filled liquid crystal depolarizers. J. Appl. Phys. **90**, 3675-3678 (2001).

[4] Wei, B. Y. et al. Liquid crystal depolarizer based on photoalignment technology. Photonics Res. **4**, 70-73 (2016).

[5] Yu, N. et al. Light Propagation with Phase Discontinuities: Generalized Laws of Reflection and Refraction. Science **334**, 333-337 (2011).

[6] Kildishev, A. V., Boltasseva, A., Shalaev, V. M. Planar Photonics with Metasurfaces. Science **339**, 1232009-1232009 (2013).

[7] Lin, D. et al. Dielectric gradient metasurface optical elements. Science **345**, 298-302 (2014).

[8] Arbabi, A. et al. Dielectric metasurfaces for complete control of phase and polarization with subwavelength spatial resolution and high transmission. Nat. Nanotechnol. **10**, 937-943 (2015).

[9] Zang, X. et al. Polarization Encoded Color Image Embedded in a Dielectric Metasurface. Adv. Mater. **30**, 1707499 (2018).

[10] Mueller, J. P. B. et al. Metasurface polarization optics: independent phase control of arbitrary orthogonal states of polarization. Phys. Rev. Lett. **118**, 113901 (2017).

[11] Zheng, G. et al. Metasurface holograms reaching 80% efficiency. Nat. Nanotechnol.

10, 308-312 (2015).

[12] Yue, F. et al. High-resolution grayscale image hidden in a laser beam. Light Sci. Appl. **7**, 17129 (2018).

[13] Khorasaninejad, M. et al. Metalenses at visible wavelengths: Diffraction-limited focusing and subwavelength resolution imaging. Science **352**, 1190-1194 (2016).

[14] Chen, W. T. et al. A broadband achromatic metalens for focusing and imaging in the visible. Nat. Nanotechnol. **13**, 220-226 (2018).

[15] Pahlevaninezhad, H. et al. Nano-optic endoscope for high-resolution optical coherence tomography in vivo. Nat. Photon. **12**, 540-547 (2018).

[16] Wang, S. et al. A broadband achromatic metalens in the visible. Nat. Nanotechnol. **13**, 227-232 (2018).

[17] Jang, M. et al. Wavefront shaping with disorder-engineered metasurfaces. Nat. Photon. **12**, 84-90 (2018).

[18] Kruk, S. et al. Broadband highly efficient dielectric metadevices for polarization control. Apl. Photonics. **1**, 030801 (2016).

[19] Fan, Q. B. et al. Autofocusing Airy beams generated by all-dielectric metasurface for visible light. Opt. Express **25**, 9285-9294 (2017).

[20] Devlin, R. C. et al. Arbitrary spin-to–orbital angular momentum conversion of light. Science **358**, 896-901 (2017).

[21] Schau, P. et al. Polarization scramblers with plasmonic meander-type metamaterials. Opt. Express **20**, 22700-22711 (2012).

[22] Fu, L. et al. Depolarization of a randomly distributed plasmonic meander

metasurface characterized by Mueller matrix spectroscopic ellipsometry. Opt. Express **24**, 28056-28064 (2016).

[23] Devlin, R. C. et al. Broadband high-efficiency dielectric metasurfaces for the visible spectrum. Proc. Natl. Acad. Sci. USA **113**, 10473-10478 (2016).

[24] Fan, Q. B. et al. Broadband Generation of Photonic Spin-Controlled Arbitrary Accelerating Light Beams in the Visible. Nano Lett. **19**, 1158-1165(2019).

Figure and caption

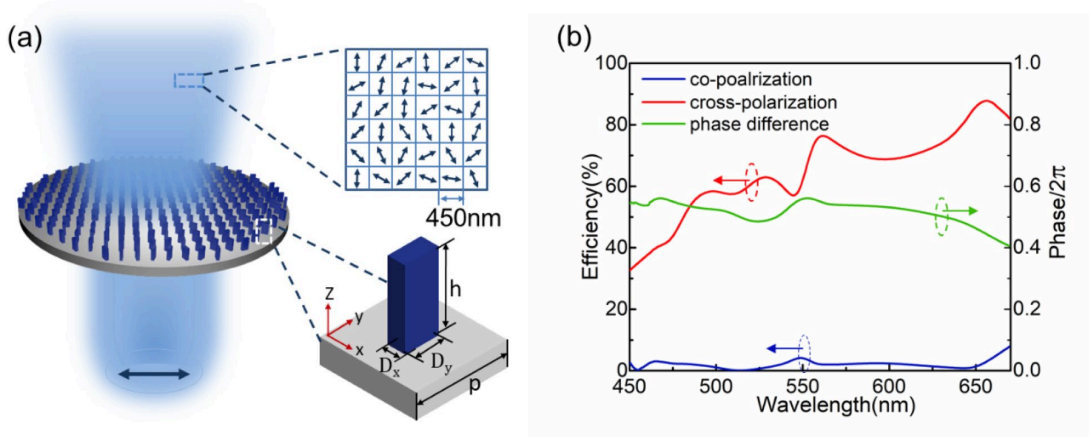

Figure 1. Schematic for the metasurface depolarizer and simulation results of a unit cell. (a) Schematic illustration of the metasurface depolarizer designed to depolarize a linearly polarized incident light. Top Inset: Exit side polarization distribution after the metasurface in a selected area. The blue arrows indicate the different output polarization states for illumination with a linearly polarized light along the *x*-axis. Bottom Inset: Oblique view of a unit cell of a rectangular TiO_2 nanopillar with a fixed height $h = 600$ nm, in-plane cross-sectional dimensions $D_x = 120$ nm, $D_y = 335$ nm and lattice constant $P = 450$ nm, on a SiO_2 substrate. (b) Simulated polarization conversion efficiency and phase difference of outgoing light as a function of wavelengths from 450 nm to 670 nm. The red and blue line represent cross-polarization and co-polarization conversion efficiency, respectively. The green line represents the phase difference between *x*- and *y*- polarized plane waves normally incident on the metasurface.

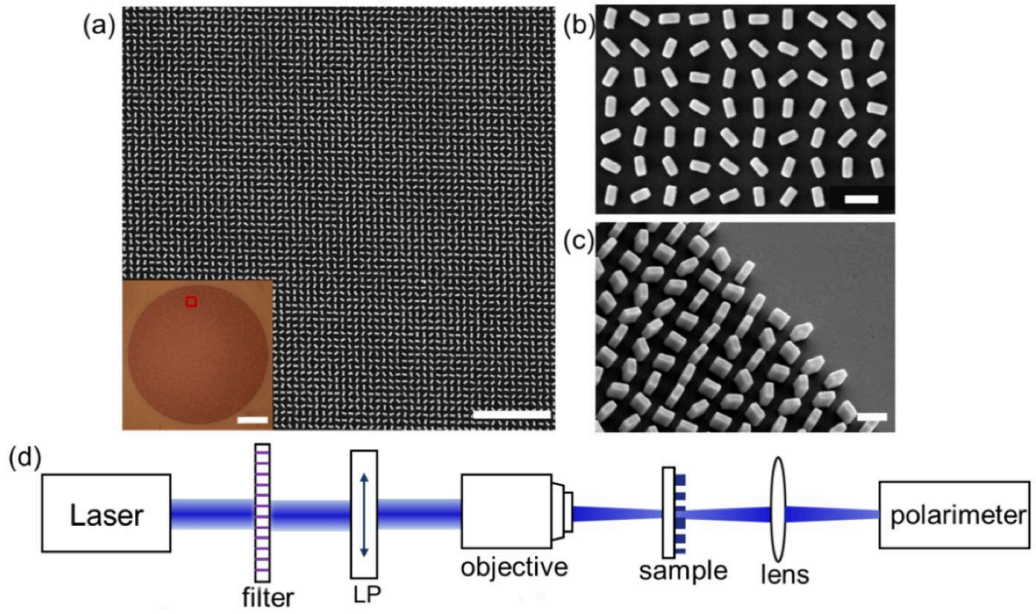

Figure 2. Fabricated sample images and experimental setup. (a) SEM image of the metasurface depolarizer. Scale bar: 5 μm. The inset shows an optical microscope image of the depolarizer. The overall diameter is 450 μm. The red frame marks the position of the SEM image. Scale bar: 100 μm. (b), (c) Magnified SEM images of the metasurface device taken at normal incidence and at a 25° tilt angle respectively. Scale bars: 500 nm. (d) Schematic drawing of measurement setup used for measuring the DOP of designed depolarizer. LP: linear polarizer.

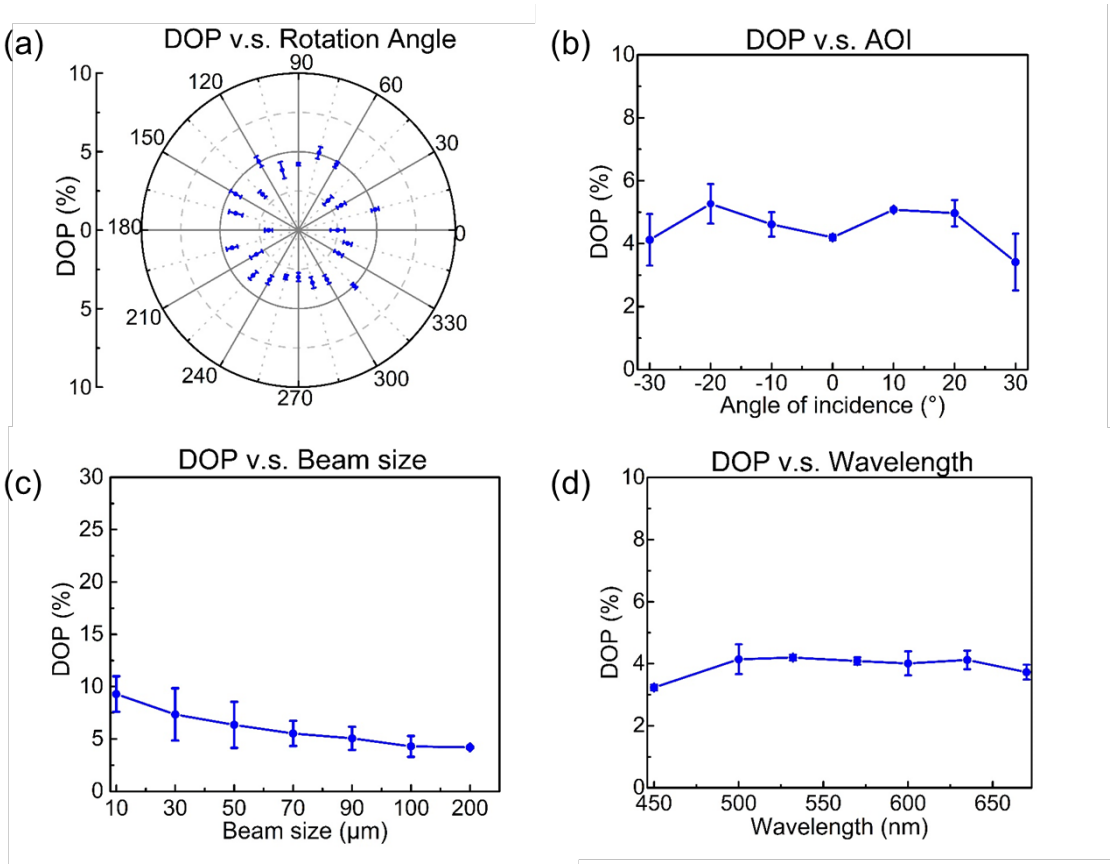

Figure 3. Experimental characterization of the metasurface depolarizer. (a) The DOP of depolarizer for different polarization directions at the wavelength of 532 nm, the beam diameter is 200 μm, and 0 degree corresponds to the *x*-polarization. (b) The DOP of depolarizer for different angles of incidence at the wavelength of 532 nm, *y*-polarization, 200 μm beam diameter. (c) The DOP of depolarizer for different beam diameters at the wavelength of 532 nm, *y*-polarization. (d) The DOP of depolarizer for different wavelengths for *y*-polarization, 200 μm beam diameter. Error bars represent the fluctuation range of DOP from repeated measurements (five in total).